

# Rhomb-dominated crystallographic preferred orientations in incipiently deformed quartz sandstones: A potential paleostress indicator for quartz-rich rocks

Jeffrey M. Rahl<sup>1</sup>, Allen J. McGrew<sup>2</sup>, Joshua A. Fox<sup>1</sup>, Joshua R. Latham<sup>2</sup>, and Tyler Gabrielson<sup>1</sup>

<sup>1</sup>Department of Geology, Washington and Lee University, Lexington, Virginia 24450, USA

<sup>2</sup>Department of Geology, University of Dayton, Dayton, Ohio 45469, USA

## ABSTRACT

We describe quartz crystallographic preferred orientations (CPOs) from incipiently deformed quartz sandstones characterized by low-intensity but unambiguous alignment of the poles to positive  $\{r\}$  and/or negative  $\{z\}$  rhombs. These distinctive CPOs appear at minimal strains and in grains with scarcely modified original detrital boundaries. We consider the hypothesis that these patterns reflect Dauphiné twinning (a  $180^\circ$  misorientation about the  $c$ -axis) that preferentially affects grains oriented with the elastically stiffer  $z$ -rhombs at high angle to the maximum principal stress direction. Twinning facilitates elastic deformation by aligning the more compliant  $r$ -rhombs at high angle to the greatest principal stress. Crystallographic maps show that about two-thirds of all grains (by area) are twinned, and untwinned grains are oriented with an  $r$ -rhombs perpendicular to the inferred shortening direction. We document this pattern from low-grade quartzite from three locations: the Eureka Quartzite of northeastern Nevada (USA); the Mesón Group of northwestern Argentina; and the Antietam Formation of the Blue Ridge of central Virginia (USA). The widespread presence of these CPOs in minimally deformed quartz rocks suggests that they may be useful in defining paleostress trajectories.

## INTRODUCTION

The alignment of crystal lattice planes during deformation (crystallographic preferred orientation, CPO) reflects various aspects of deformation, including strain magnitude and geometry, strain path, temperature, and/or water content (e.g., Schmid and Casey, 1986). The mineral quartz figures prominently in such studies due to its abundance and importance in determining the strength of the continental crust (e.g., Kohlstedt et al., 1995). Many quartz studies emphasize  $c$ -axis distributions, which are measurable using a petrographic microscope with a universal stage and are interpretable in terms of deformation history. The advent of electron backscatter diffraction (EBSD) has made analysis of other crystallographic orientations routine, enabling investigation of additional aspects of quartz deformation (Prior et al., 1999).

Here, we document a little-described quartz texture, characterized by near-uniform  $[c]$  and  $\langle a \rangle$  distributions but with CPOs defined by the poles to the rhomb planes,  $\{r\}$  and  $\{z\}$ . Quartzite from three geologic settings display this pattern, suggesting that it may occur widely in incipiently deformed quartz-rich rocks. We interpret this pattern to record Dauphiné twinning, which can be described as a  $180^\circ$  rotation around the  $c$ -axis that transposes the positive and negative rhombs and changes the polarity of  $\langle a \rangle$  without

affecting  $[c]$  (Thomas and Wooster, 1951). These twins are common in a variety of natural samples, including sedimentary rocks (e.g., Olierook et al., 2014), mylonites (Lloyd, 2004; Pehl and Wenk, 2005; Menegon et al., 2011), and migmatites (Levine et al., 2016). Because the elastic properties of quartz are anisotropic (e.g., Ohno et al., 2006), with the poles to the negative rhomb  $\{z\}$  faces nearly twice as stiff as those to the positive rhombs  $\{r\}$ , Dauphiné twinning facilitates elastic strain by aligning the more compliant poles to  $\{r\}$  with the greatest principal stress direction (Fig. 1). Mechanically induced Dauphiné twinning has long been observed experimentally (e.g., Thomas and Wooster, 1951; Tullis, 1970; Wenk et al., 2009), but it has not previously been

documented as the main CPO-producing mechanism in natural samples. Here we document Dauphiné twinning in quartzite and demonstrate alignment of the poles to the  $\{r\}$  rhombs parallel to weakly developed intracrystalline principal strain directions where known. These examples suggest that CPOs produced by Dauphiné twinning hold potential as a paleostress indicator.

## SAMPLE MATERIALS

We obtained CPO data from incipiently deformed orthoquartzites from three units: the Eureka Quartzite in northeastern Nevada (USA) (Camilleri, 2010), the Mesón Group of northwestern Argentina (Augustsson et al., 2011), and the Antietam Formation of the Virginia Blue Ridge (USA) (Schwab, 1970). The tectonic histories of these units are broadly similar, with passive margin deposition followed by contraction in a deforming foreland. The Ordovician Eureka Quartzite samples are very well-sorted, with rounded quartz grains  $\sim 200 \mu\text{m}$  diameter in thin section. Many grains appear to preserve near-primary textures, although undulose extinction and basal subgrains are evident locally. Burial temperatures for the studied Eureka samples did not exceed  $300\text{--}450^\circ\text{C}$  (Howland et al., 2016). The Mesón Group samples consist of well-sorted quartz grains and sparse lithic clasts  $\sim 200 \mu\text{m}$  diameter, with some grains  $>1000 \mu\text{m}$  in diameter. The grains are only slightly deformed, locally showing weak undulose extinction, and rare subgrains and

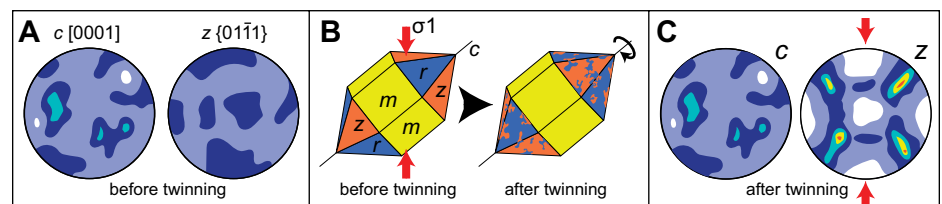


**Figure 1. A:** Cartoon pole figures of contoured quartz crystallographic data from undeformed rock, showing uniform distributions for  $c$ -axis and negative rhombs  $\{z\}$ . **B:** Sketch of quartz crystal showing  $c$ -axis and prism  $\{m\}$ , yellow, positive rhomb  $\{r\}$ , blue, and negative rhomb  $\{z\}$ , orange faces. Mechanical Dauphiné twinning occurs when greatest principal stress (red arrows) is perpendicular to  $\{z\}$ . **C:** As A, after mechanical Dauphiné twinning. Warm colors in pole figures indicate greater concentrations of crystallographic directions.

deformation lamellae. The Cambrian Antietam Formation preserves well-rounded, well-sorted quartz grains ~400  $\mu\text{m}$  diameter with abundant deformation lamellae locally warped by undulose extinction. Most Antietam Formation samples show evidence for only minor deformation, such as locally developed subgrains or serrate grain boundaries indicating incipient bulge nucleation. Some grains contain needle-like rutile inclusions that are folded or boudinaged and record small finite strains (see below). Quartz opening angle thermometry (Law, 2014) applied to a strained sample indicates deformation at ~325  $^{\circ}\text{C}$ . Representative photomicrographs for all units are available in the GSA Data Repository (Fig. DR1)<sup>1</sup>.

## METHODS

Polished thin sections of 17 samples oriented perpendicular to bedding were analyzed using EBSD at Washington and Lee University (Lexington, Virginia) (4, 3, and 11 samples from the Eureka Quartzite, Mesón Group, and Antietam Formation respectively). Data were collected on an Oxford EBSD system with Aztec software running on a Zeiss EVO-MA 15 scanning electron microscope in variable pressure mode, with an accelerating voltage of 25 kV, a probe current of 20 nA, and a working distance between 21 and 28 mm. CPO data were collected in a series of 500  $\mu\text{m}$  x 375  $\mu\text{m}$  scan regions on a relatively coarse grid (30–50  $\mu\text{m}$  step size) that enabled identification of grains over large areas (median = 81  $\text{mm}^2$ ). Smaller areas scanned at 4  $\mu\text{m}$  resolution (see below) established the scale independence of the results. Data were processed using the MTEX toolbox version 4.5 (Hielscher and Schaeben, 2008). Individual grains were reconstructed using a 10 $^{\circ}$  misorientation for quartz, with Dauphiné twin boundaries identified by a 60 $^{\circ}$   $\pm$  2.5 $^{\circ}$  misorientation around  $[c]$ . Low-quality EBSD observations (mean angular deviation >1.0) were removed from the analysis, and grains were required to contain at least five contiguous points to guard against misindexing artifacts. Contoured pole figures (Figs. 2 and 3) are based on all data within grains, although results are similar if plotted using one point per grain.

## CRYSTALLOGRAPHIC PREFERRED ORIENTATIONS IN INCIPIENTLY DEFORMED QUARTZITE

As expected for minimally strained rocks, the samples from all settings show little to no CPO in  $[c]$  and  $\langle a \rangle$ , with contoured plots of  $[c]$  distributions showing maxima of less than two multiples of uniform density and even weaker

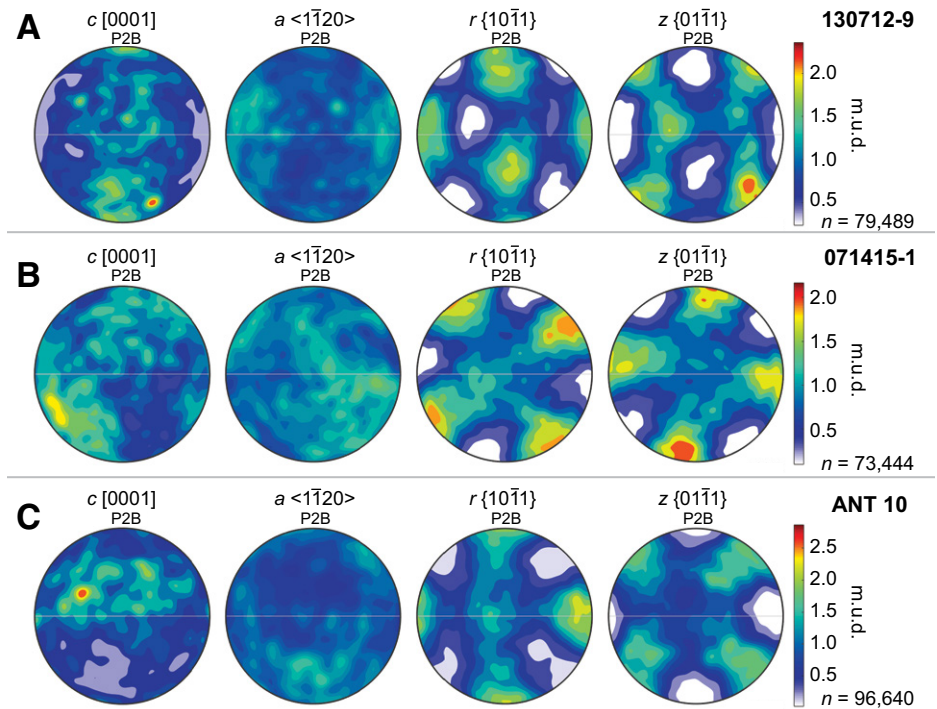


**Figure 2.** Pole figures of contoured quartz crystallographic data from representative quartzite samples from Eureka Quartzite (northeastern Nevada, USA) (A), Mesón Group (northwestern Argentina) (B), and Antietam Formation (Blue Ridge of central Virginia, USA) (C);  $n$ —total number of analyzed data. Figures are oriented with pole to bedding plane (P2B) along N-S axis and arbitrary direction aligned E-W. Orientations shown are for  $[0001]$  ( $c$ -axis),  $\langle 11\bar{2}0 \rangle$  ( $a$ -axis),  $\{10\bar{1}1\}$  (positive rhomb,  $r$ ), and  $\{01\bar{1}1\}$  (negative rhomb,  $z$ ) directions. m.u.d.—multiples of uniform density.

$\langle a \rangle$  distributions (Fig. 2; Fig. DR2). However, we find discernible CPOs of the poles to  $\{r\}$  and  $\{z\}$  with two or three nearly orthogonal local maxima. Maxima in  $\{r\}$  and  $\{z\}$  are typically ~60 $^{\circ}$  to each other, as expected from crystal symmetry. In some cases, the subsidiary maxima are merged into small-circle girdle distributions, especially evident in the  $\{z\}$  poles (Figs. 2 and 3).

Quartz CPO fabrics are typically attributed to activity of slip systems that rotate crystallographic orientations. However, these processes are not significant in our samples because: (1) known quartz slip systems typically align  $[c]$  more strongly than rhombs; and (2) the rocks preserve evidence of only minor crystal-plastic strain, such as a grain-shape preferred orientation or recrystallization. Rather, we hypothesize that the observed CPOs reflect post-deposition Dauphiné twinning. The uniform  $c$ -axis patterns support the idea that deposition randomized all crystallographic directions. While individual grains may preserve twins inherited from the source area, many must have formed in situ to create the observed CPOs.

Dauphiné twins may form as quartz cools from the  $\beta$ -quartz (hexagonal) to the  $\alpha$ -quartz (trigonal) stability field (Wenk et al., 2009) or as grains grow by grain boundary migration (Piazolo et al., 2005), but the inferred maximum temperatures in these rocks (<450  $^{\circ}\text{C}$ ) are too

low for these processes to have operated post-depositionally. We favor a third mechanism in which the twins form in response to differential stress. Thomas and Wooster (1951) first argued that anisotropy in the elastic properties of quartz (Fig. 4D) will cause quartz to twin when stressed, in order to maximize the elastic energy stored within the crystal (see Barton and Wenk [2007] for detail on the twinning mechanism). Experimental work demonstrates that twinning aligns the softer positive rhombs  $\{r\}$  normal to the greatest principal stress, beginning at deviatoric stresses as low as 50–80 MPa (Wenk et al., 2007).

Grains initially oriented with the less-compliant  $\{z\}$  faces nearly perpendicular to the greatest principal stress direction should be most prone to twinning. Although we lack *a priori* knowledge of the detailed stress history, we argue that coaxial and/or very small intracrystalline strains may serve as a proxy for the stress orientations. Mitra (1978) demonstrated that needle-like rutile inclusions within quartz may serve as effective strain markers. Needles oriented parallel to directions of extension appear broken and boudinaged, whereas others in shortening directions become kinked and folded. We measured strain on three samples from the Antietam Formation using rutile inclusions on three mutually orthogonal polished thin sections. Rutile-bearing quartz grains were photographed

<sup>1</sup>GSA Data Repository item 2017047, sample photomicrographs, crystallographic data from additional samples, and a figure illustrating the strain analysis methods, is available online at <http://www.geosociety.org/datarepository/2017/> or on request from [editing@geosociety.org](mailto:editing@geosociety.org).

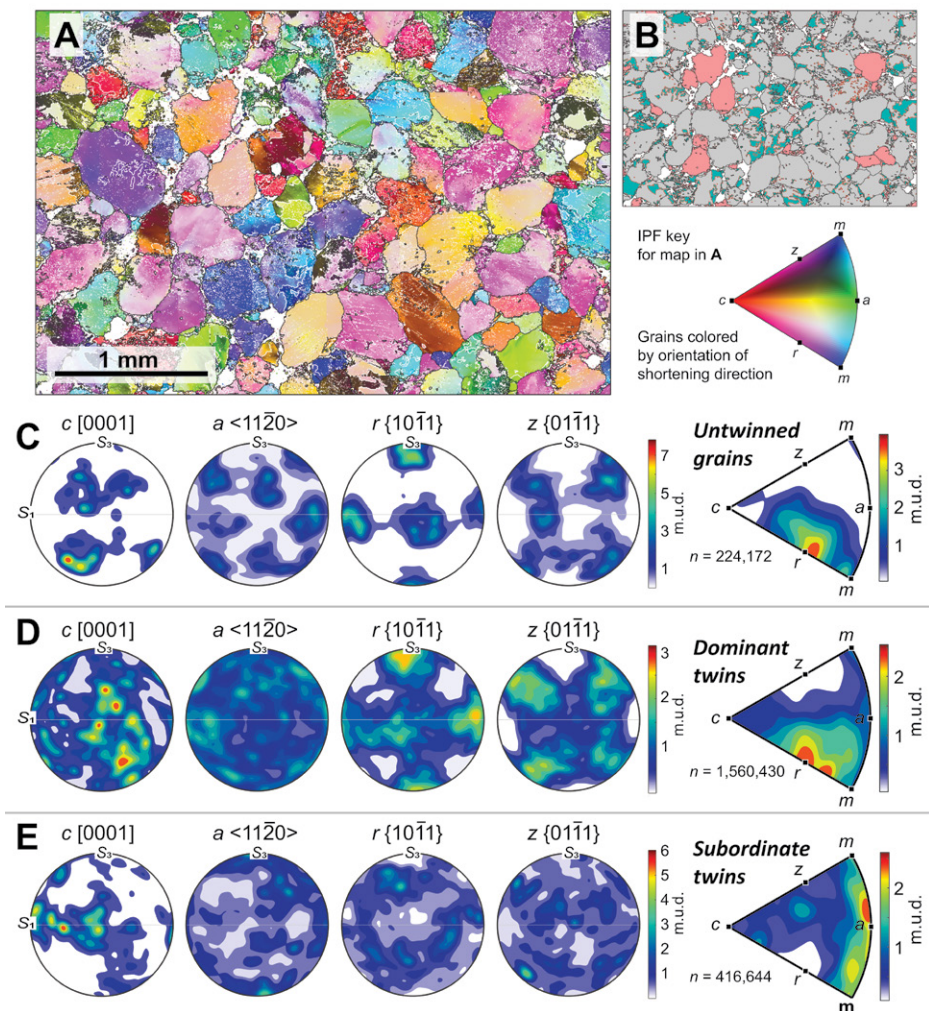


**Figure 3. A:** Quartz crystallographic map from sample ANT 10 of Antietam Formation, collected on rectangular grid with  $4\ \mu\text{m}$  step size. Data are colored according to inverse pole figure (IPF) (right) showing maximum shortening direction inferred from strain analysis in crystallographic reference frame for quartz (see text for details). Grain boundaries are black; white lines indicate Dauphiné twin boundaries. **B:** Same area as in A, but showing un-twinned grains (pink), dominant twins (gray), subordinate twins (teal), and twin boundaries (red). **C–E:** Pole figures of contoured quartz crystallographic data, for data from un-twinned grains (C), the volumetrically dominant twins (D), and the subordinate twins (E). Contoured data include all collected data ( $n$ —number of observations). Pole figures are oriented with inferred shortening direction ( $S_3$ ) on N-S axis and maximum extension direction ( $S_1$ ) aligned E-W. Orientations shown are for  $[0001]$  ( $c$ -axis),  $\langle 11\bar{2}0 \rangle$  ( $a$ -axis),  $\{10\bar{1}1\}$  (positive rhomb,  $r$ ), and  $\{01\bar{1}1\}$  (negative rhomb,  $z$ ) directions. Inverse pole figures for shortening direction are shown to right. m.u.d.—multiples of uniform density.

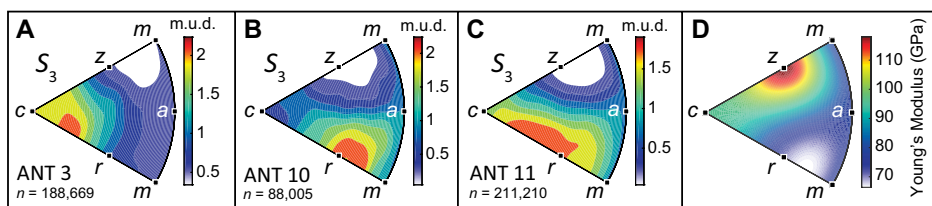


**Figure 4. A–C:** Inverse pole figures showing contoured maximum shortening axes ( $S_3$ ) relative to quartz crystallographic directions for three samples; m.u.d.—multiples of uniform density;  $n$ —number of observations. Note dispersion of grains oriented with negative rhombs perpendicular to maximum shortening direction, supporting the hypothesis that twinning preferentially affects such grains. Maxima near  $[c]$  for sample ANT 3 (A) probably reflects activation of basal  $\langle a \rangle$  slip system (Schmid and Casey, 1986) that somewhat swamps rhomb signal. **D:** Young's modulus at  $374\ ^\circ\text{C}$  for quartz, showing higher values (elastically stiffer) around negative rhomb  $\{z\}$  direction (elastic parameters from Ohno et al., 2006). m.u.d.—multiples of uniform density.

at high magnification ( $40\times$ ), and fragments were digitized using the ImageJ software (<https://imagej.nih.gov/ij/>). The stretch (ratio of final length to initial length) and orientation were determined for each observation, and a best-fit ellipsoid was calculated using a least-squares approach for a minimum of 85 observations per sample. (Additional methodological details are in the Data Repository). The observed intracrystalline strains are small, with maximum stretch values  $S_1 < 1.14$  and  $S_1/S_3$  ratios between 1.22 and 1.38, suggesting that the determined strain directions provide reasonable proxies for the principal stress directions.

We document twinning microstructure with crystallographic maps on square grids with step sizes of  $4$  or  $5\ \mu\text{m}$ . We focus on sample ANT 10 of the Antietam Formation (Fig. 3), although the results are representative of those obtained on other samples (see Data Repository Figs. DR2 and DR3). Twin boundaries show an interpenetrating geometry characteristic of Dauphiné twinning (Judd, 1888), implying that these features are real rather than an analytical artifact. Dauphiné twinned grains are dispersed throughout the sample forming  $\sim 60\%$ – $70\%$  of the grains by area.

We rotated the crystallographic data into a reference frame defined by the measured three-dimensional strain axes and subdivided it based on its twinning (Figs. 3C–3E). CPO data from un-twinned grains show clear maxima in the rhombs with  $\{r\}$  poles parallel to the maximum shortening direction. For grains with twins, a question arises as to which of the two domains represents the initial orientation and which is its twin. We hypothesize that the twinned domains will become dominant and thus will be more favorably oriented in the inferred stress regime relative to the subordinate domains. For each twinned grain, we calculated the relative area of each domain to define the *dominant* (larger) and *subordinate* (smaller) twins. The CPO of the dominant twins yields a strikingly similar but more diffuse version of that for the un-twinned grains, whereas the subordinate twins show a complementary but much weaker pattern characterized by voids near  $\{r\}$ , supporting the idea that these are mostly relict grains in elastically stiffer orientations. This is an imperfect method for separating the twinned from the original orientations because the dominant twins in some grains are oriented comparably to the subordinate twins in others. Nevertheless, the similarity between the CPOs of the un-twinned grains and the dominant twins occurs in all samples, including cases where we have not performed strain analysis.

Inverse pole figures illustrate the relationship between the maximum shortening direction and the crystallographic distributions (Figs. 4A–4C). In each case, the maximum shortening direction is dispersed away from the stiffer negative

rhombs  $\{z\}$  orientations, and in most cases it is aligned preferentially near the more compliant  $r$ -pole positions. The inverses of these non-random distributions bear a striking similarity to that of the Young's modulus of quartz (Fig. 4D), arguing for a relationship between its elastic properties and the observed CPOs.

## DISCUSSION AND CONCLUSIONS

We observe rhomb-dominated quartz CPOs from three settings, implying that these patterns may be common in weakly deformed quartzites. The uniform distributions of  $\{c\}$  and  $\langle a \rangle$  and the weakly strained nature of these samples argue against reorientation by dislocation creep. Instead, we infer that mechanically driven Dauphiné twinning produces alignment of the more elastically compliant poles to the positive rhomb parallel to the greatest principal stress direction. Untwinned grains and the dominant twins in twinned grains are well-oriented for elastic distortion; conversely, the subordinate twins in twinned grains tend to be in stiffer orientations. Similarity between the distributions of untwinned grains and those of the dominant twins implies that the twinning process efficiently reorganizes the bulk of each crystal and raises the possibility that some untwinned grains may have been completely twinned from a stiff initial orientation.

Our results support the idea that the distribution of Dauphiné twins may form the basis of a new paleostress tool, partially analogous to calcite twin analysis (Burkhard, 1993). Given the widespread occurrence of quartzite in orogenic belts, such a tool could be widely applicable to the reconstruction of paleostress trajectories. However, important issues remain—the most significant being how to determine which of the symmetrically requisite  $\{r\}$  maxima best correlates with the greatest principal stress. Can some aspect of the microstructure or CPO data (such as small differences in peak intensity, or the presence or absence of small-circle distributions) aid in constraining the orientations and relative magnitudes of each of the three principal stress directions? What is the sensitivity and memory of the twinning process? Despite these important caveats, Dauphiné twinning is clearly a common response to stress in low-grade, slightly deformed quartzites, and future investigation of these textures holds intriguing potential to reveal paleostress fields.

## ACKNOWLEDGMENTS

This material is based upon work supported by the National Science Foundation under grant NSF-REU 1358987 to the Keck Geology Consortium. We are grateful for reviews from Andrew Cross, Stephen Laubach, Geoff Lloyd, Luca Menegon, Luiz Morales, Nick Timms, and an anonymous reviewer

that improved our presentation. Further support was provided by a Lenfest Grant from Washington and Lee University to Rahl, Summer Research Scholar Grants from Washington and Lee University to Gabrielson and Fox, and funds from the University of Dayton and Washington and Lee University.

## REFERENCES CITED

- Augustsson, C., Rüsing, T., Adams, C.J., Chmiel, H., Kocabayoglu, M., Büld, M., Zimmermann, U., Berndt, J., and Kooijman, E., 2011, Detrital quartz and zircon combined: The production of mature sand with short transportation paths along the Cambrian West Gondwana margin, northwestern Argentina: *Journal of Sedimentary Research*, v. 81, p. 284–298, <https://doi.org/10.2110/jsr.2011.23>.
- Barton, N.R., and Wenk, H.-R., 2007, Dauphiné twinning in polycrystalline quartz: Modelling and Simulation in Materials Science and Engineering, v. 15, p. 369–384, <https://doi.org/10.1088/0965-0393/15/3/013>.
- Burkhard, M., 1993, Calcite twins, their geometry, appearance and significance as stress-strain markers and indicators of tectonic regime: A review: *Journal of Structural Geology*, v. 15, p. 351–368, [https://doi.org/10.1016/0191-8141\(93\)90132-T](https://doi.org/10.1016/0191-8141(93)90132-T).
- Camilleri, P., 2010, Geologic map of the northern Pequo Mountains, Elko County, Nevada: Nevada Bureau of Mines and Geology Map 172, scale 1:48,000.
- Hielscher, R., and Schaeben, H., 2008, A novel pole figure inversion method: Specification of the MTEX algorithm: *Journal of Applied Crystallography*, v. 41, p. 1024–1037, <https://doi.org/10.1107/S0021889808030112>.
- Howland, C., Manon, M.R.F., Rahl, J.M., and McGrew, A.J., 2016, High thermal gradient in the upper plate of a core complex, determined by calcite-dolomite and RSCM thermometry, Pequo Mountains, NV: *Geological Society of America Abstracts with Programs*, v. 48, no. 2, <https://doi.org/10.1130/abs/2016NE-272907>.
- Judd, J.W., 1888, On the development of a lamellar structure in quartz-crystals by mechanical means: *Mineralogical Magazine*, v. 8, p. 1–9, <https://doi.org/10.1180/minmag.1888.008.36.01>.
- Kohlstedt, D.L., Evans, B., and Mackwell, S.J., 1995, Strength of the lithosphere: Constraints imposed by laboratory experiments: *Journal of Geophysical Research*, v. 100, p. 17,587–17,602, <https://doi.org/10.1029/95JB01460>.
- Law, R.D., 2014, Deformation thermometry based on quartz  $c$ -axis fabrics and recrystallization microstructures: A review: *Journal of Structural Geology*, v. 66, p. 129–161, <https://doi.org/10.1016/j.jsg.2014.05.023>.
- Levine, J.S., Mosher, S., and Rahl, J.M., 2016, The role of subgrain boundaries in partial melting: *Journal of Structural Geology*, v. 89, p. 181–196, <https://doi.org/10.1016/j.jsg.2016.06.006>.
- Lloyd, G.E., 2004, Microstructural evolution in a mylonitic quartz simple shear zone: The significant roles of dauphiné twinning and misorientation, *in* Alsop, G.I., et al., eds., *Flow Processes in Faults and Shear Zones*: Geological Society of London Special Publication 224, p. 39–61, <https://doi.org/10.1144/GSL.SP.2004.224.01.04>.
- Menegon, L., Piazzolo, S., and Pennacchioni, G., 2011, The effect of Dauphiné twinning on plastic strain in quartz: Contributions to Mineralogy and Petrology, v. 161, p. 635–652, <https://doi.org/10.1007/s00410-010-0554-7>.
- Mitra, S., 1978, Microscopic deformation mechanisms and flow laws in quartzites within the South Mountain anticline: *The Journal of Geology*, v. 86, p. 129–152, <https://doi.org/10.1086/649660>.
- Ohno, I., Harada, K., and Yoshitomi, C., 2006, Temperature variation of elastic constants of quartz across the  $\alpha$ - $\beta$  transition: Physics and Chemistry of Minerals, v. 33, p. 1–9, <https://doi.org/10.1007/s00269-005-0008-3>.
- Olierook, H.K., Timms, N.E., and Hamilton, P.J., 2014, Mechanisms for permeability modification in the damage zone of a normal fault, northern Perth Basin, Western Australia: *Marine and Petroleum Geology*, v. 50, p. 130–147, <https://doi.org/10.1016/j.marpetgeo.2013.10.012>.
- Pehl, J., and Wenk, H.-R., 2005, Evidence for regional Dauphiné twinning in quartz from the Santa Rosa mylonite zone in Southern California: A neutron diffraction study: *Journal of Structural Geology*, v. 27, p. 1741–1749, <https://doi.org/10.1016/j.jsg.2005.06.008>.
- Piazzolo, S., Prior, D.J., and Holness, M.D., 2005, The use of combined cathodoluminescence and EBSD analysis: A case study investigating grain boundary migration mechanisms in quartz: *Journal of Microscopy*, v. 217, p. 152–161, <https://doi.org/10.1111/j.1365-2818.2005.01423.x>.
- Prior, D.J., et al., 1999, The application of electron backscatter diffraction and orientation contrast imaging in the SEM to textural problems in rocks: *The American Mineralogist*, v. 84, p. 1741–1759, <https://doi.org/10.2138/am-1999-11-1204>.
- Schmid, S.M., and Casey, M., 1986, Complete fabric analysis of some commonly observed quartz  $c$ -axis patterns, *in* Hobbs, B.E., and Heard, H.C., eds., *Mineral and Rock Deformation: Laboratory Studies (The Paterson Volume)*: American Geophysical Union Geophysical Monograph 36, p. 263–286, <https://doi.org/10.1029/GM036p0263>.
- Schwab, F.L., 1970, Origin of the Antietam Formation (Late Precambrian?–Lower Cambrian), central Virginia: *Journal of Sedimentary Research*, v. 40, p. 354–366.
- Thomas, L.A., and Wooster, W.A., 1951, Piezocrescence—The growth of Dauphiné twinning in quartz under stress: *Proceedings of the Royal Society of London A: Mathematical, Physical and Engineering Sciences*, v. 208, p. 43–62, <https://doi.org/10.1098/rspa.1951.0143>.
- Tullis, J., 1970, Quartz: Preferred orientation in rocks produced by Dauphiné twinning: *Science*, v. 168, p. 1342–1344, <https://doi.org/10.1126/science.168.3937.1342>.
- Wenk, H.-R., Bortolotti, M., Barton, N., Oliver, E., and Brown, D., 2007, Dauphiné twinning and texture memory in polycrystalline quartz. Part 2: *In situ* neutron diffraction compression experiments: *Physics and Chemistry of Minerals*, v. 34, p. 599–607, <https://doi.org/10.1007/s00269-007-0174-6>.
- Wenk, H.-R., Barton, N., Bortolotti, M., Vogel, S.C., Voltolini, M., Lloyd, G.E., and Gonzalez, G.B., 2009, Dauphiné twinning and texture memory in polycrystalline quartz. Part 3: Texture memory during phase transformation: *Physics and Chemistry of Minerals*, v. 36, p. 567–583, <https://doi.org/10.1007/s00269-009-0302-6>.

Manuscript received 4 August 2017

Revised manuscript received 17 November 2017

Manuscript accepted 19 November 2017

Printed in USA